Originally published as:

Geyer, H., Hartung, E., Mages, H.W., Weise, C., Belužić, R., Vugrek, O., Jonjić, S., Kroczek, R.A., Voigt, S.
Cytomegalovirus Expresses the Chemokine Homologue vXCL1 Capable of Attracting XCR1+ CD4- Dendritic Cells
(2014) Journal of Virology, 88 (1), pp. 292-302.

DOI: 10.1128/JVI.02330-13

Cytomegalovirus expresses the chemokine homologue vXCL1 capable of attracting XCR1^{+}CD4^{-} dendritic cells

Running title: vXCL1 attracts XCR1^{+} DC

Keywords: CMV, C-chemokine, viral homologue, vXCL1, XCR1, dendritic cells

Henriette Geyer[a*], Evelyn Hartung[b*], Hans Werner Mages[b], Christoph Weise[c], Robert Belužić[d], Oliver Vugrek[d], Stipan Jonjić[e], Richard A. Kroczek[b], Sebastian Voigt[a,#]

[a]Virology and [b]Molecular Immunology, Robert Koch Institute, Nordufer 20, 13353 Berlin, Germany

[c]Institute of Chemistry and Biochemistry, Freie Universität Berlin, Thielallee 63, 14195 Berlin, Germany

[d]Department of Molecular Medicine, Ruđer Bošković Institute, Bijenička 54, 10000 Zagreb, Croatia

[e]Department of Histology and Embryology, University of Rijeka, B. Branchetta 20, 51000 Rijeka, Croatia

*Authors contributed equally.

[#]Corresponding author. Mailing address: Robert Koch Institute, FG12, Nordufer 20, 13353 Berlin, Germany, Phone: +49-30-187542271. Fax: +49-30-18107542271. Email: sebastian.voigt@charite.de

Word count abstract: 171

Word count text: 5325

Abstract

Cytomegaloviruses (CMV) have developed various strategies to escape the immune system of the host. One strategy involves the expression of virus-encoded chemokines to modulate the host chemokine network. We have identified in the English isolate of rat CMV (murid herpesvirus 8; MuHV8) an open reading frame encoding a protein homologous to the chemokine XCL1, the only known C-chemokine. Viral XCL1 (vXCL1), a glycosylated protein of 96 amino acids, can be detected 13 hours post infection in the supernatant of MuHV8-infected rat embryo fibroblasts. vXCL1 exclusively binds to $CD4^-$ rat dendritic cells (DC), a DC subset that expresses the corresponding chemokine-receptor XCR1. Like endogenous rat XCL1, vXCL1 selectively chemoattracts $XCR1^+$ $CD4^-$ DC. Since $XCR1^+$ DC in mice and humans have been shown to excel in antigen cross-presentation and thus in the induction of cytotoxic $CD8^+$ T lymphocytes, the virus has apparently hijacked this gene to subvert cytotoxic immune responses. The biology of vXCL1 offers an interesting opportunity to study the role of XCL1 and $XCR1^+$ DC in the cross-presentation of viral antigens.

Introduction

Chemokines are small chemotactic cytokines which are classified into the CXC-, CC-, C-, and CX_3C-subfamilies based on the position of conserved cysteine residues at their N-terminus. The C-chemokine subfamily is characterized by only one cysteine at the N-terminus and contains only one member, XCL1. In humans, two variants (XCL1 and XCL2) that differ by two amino acids have been reported (1). XCL1, a glycosylated 93 amino-acid mature protein (2), has been shown to be secreted by activated NK cells (3) and $CD8^+$ T cells (4). Murine and human XCL1 specifically

chemoattract a particular subset of dendritic cells (DC) which express XCR1, the only receptor for XCL1 (5, 6). $XCR1^+$ DC excel in antigen cross-presentation, a process in which extracellular antigens are presented by MHC class I molecules to $CD8^+$ T cells (7-9). Antigen cross-presentation is thought to play a major role in the immune defense against viruses that do not directly infect DC (10, 11). The XCL1-XCR1 interaction facilitates the communication between $XCR1^+$ DC and activated $CD8^+$ T cells or NK cells secreting XCL1 during infection and thereby promotes the differentiation of $CD8^+$ T cells into cytotoxic effector cells (reviewed in (12)).

Cytomegaloviruses (CMV) belong to the *herpesviridae*, a family of large double-stranded DNA viruses that infect a broad spectrum of species and cause lifelong infections in their respective hosts (13). In order to survive successfully and establish latency, CMV have developed various strategies to escape different immune defense mechanisms. One strategy involves the expression of virus-encoded chemokines that interfere with the host chemokine network. It has been speculated that these genes were obtained from the host genome during coevolution and that they contribute to viral dissemination and maintenance (14).

So far, CXC- and CC-chemokines have been described for rodent, primate and human CMV (HCMV). Three chemokine-like genes have been described in the HCMV genome: *UL128*, *UL146* and *UL147* (15, 16). *UL146* and *UL147* encode the proteins vCXC-1 and vCXC-2, respectively. Only vCXC-1 has been shown to represent a functional chemokine since it binds to the chemokine receptors CXCR1 and CXCR2 and induces migration of neutrophils to the site of infection (17), a process that has been suggested to facilitate viral dissemination. Whereas one study showed that the *UL128* gene product pUL128 blocked migration and induced down-regulation of chemokine receptors in monocytes (18), another report demonstrated a

contrary effect for pUL128 as it induced migration of peripheral blood mononuclear cells (19), a discrepancy that might be due to N-terminal modifications of the chemokines resulting in different chemotactic behavior. It has also been reported that MuHV-2 r129 induces migration of immune cells (20). *UL146* and *UL147* are restricted to genomes of primate CMVs and have no sequence counterparts in rodent CMV.

CC-chemokines have been characterized in rodent CMV, e.g., Maastricht rat CMV (RCMV; murid herpesvirus 2 (MuHV2))-encoded *rck-3* (21) and *rck-2* (22), murine CMV (MCMV; MuHV1)-encoded chemokine *mck-2* (23) and English RCMV (MuHV8)-encoded *eck-2* (24). Amongst these chemokines, MCK-2 is the most extensively studied viral chemokine. MCK-2 has been shown to enhance recruitment of inflammatory monocytes to the site of infection (25). Attracted monocytes inhibit $CD8^+$ T cell activation and cytotoxicity which results in slower viral clearance (26).

Our analysis of the MuHV8 genome (27) revealed the presence of a C-chemokine, located at nucleotide positions 186261 to 186608 towards the right terminus that, to our knowledge, is the first viral C-chemokine to be reported. The gene product, designated vXCL1, shares extensive homology with the C-chemokine XCL1 of rat, mouse, and human. Here, we show that vXCL1 carries a cleavable N-terminal signal sequence that allows secretion from infected cells. Furthermore, vXCL1 functionally resembles host XCL1 since it binds to $XCR1^+CD4^-$ DC and selectively chemoattracts this particular cell subset. Since murine and human XCR1-expressing DC excel in antigen cross-presentation, vXCL1 might attract this rat DC subset in order to manipulate and disable this important branch of the immune defense.

Materials and Methods

Viruses and cell culture. MuHV8 was propagated on REF maintained in DMEM supplemented with 2 % fetal bovine serum, 2 mM L-glutamine and 100 µg/ml penicillin/streptomycin. To determine vXCL1 mRNA and protein expression kinetics, REF were treated two hours prior to infection or three hours prior to harvest with 100 µg/ml cycloheximide (Sigma-Aldrich, Taufkirchen, GER) or 5 µg/ml Brefeldin A (Sigma-Aldrich), respectively. In order to generate a MuHV8 mutant lacking *vxcl1*, a shuttle vector was generated containing 1.5 kbp of upstream and downstream sequences of *vxcl1* using e155 forward (5'-TAGCCGAGACTTCGCACTTC-3') and reverse (5'-GCCGGAGAGGTGTTTGATTC-3') primers, and e159 forward (5'-TTCACTACCGAGTGGAACTG-3') and reverse (5'-GTTCGCAACGAGACCGTCAG-3') primers, respectively. The *vxcl1* ORF in this shuttle vector was exchanged by a green fluorescent protein (GFP) expression cassette flanked by two LoxP sites. To knockout the *vxcl1* ORF within the MuHV8 genome, REF were co-transfected with 2 µg of linearized shuttle vector and 2 µg MuHV8 virion DNA using Polyfect according to manufacturer's recommendations. *vxcl1* knockout virus was identified by GFP fluorescence and isolated by limiting dilution.

RNA isolation, cDNA synthesis, PCR, 3'- and 5'-RACE. Isolation of viral and cellular RNA was carried out with the RNeasy Mini Isolation Kit according to the manufacturer's instructions (Qiagen, Hilden, GER). $2 \cdot 10^6$ cells were used per RNA isolation column and remaining DNA contaminations were removed by a 30 min digest with 20 units of Turbo-DNase (Ambion, Darmstadt, GER) on the column. For cDNA generation, 1 µg of RNA was incubated for 1 h at 45°C with the following components: 200 U RevertAid™ H minus reverse transcriptase, 5 µM oligo(dT)18

primer, 1x reaction buffer, 1 mM dNTP and 20 U RiboLock RNase inhibitor (Fermentas, St. Leon-Rot, GER). To exclude DNA contaminations present in the RNA preparation, cDNA synthesis was additionally carried out with the same components but lacking reverse transcriptase. The reaction was terminated by heating the mixture for 10 min at 70°C. 1 µl of the reaction mixture was applied in a PCR reaction using the Platinum Taq DNA polymerase (Invitrogen, Karlsruhe, GER) to amplify cDNA with gene-specific primers according to the manufacturer's recommendations. The primer pair *vXCL1 universal fwd* (5'-ATGCGAGCGGTAATCTTTG-3') and *vXCL1 universal rev* (5'-CAGGAACCTGCGTGGGAATA-3') was used for the amplification of vXCL1 mRNA, the primer pair *c-myc fwd* (5'-GCCAGAGGAGGAACGAGCT-3') and *c-myc rev* (5'-GGGCCTTTTCATTGTTTTCCA-3') for the amplification of c-myc mRNA, and the primers *GAPDH fwd* (5'-GGTCGGTGTGAACGGATTTG-3') and *GAPDH rev* (5'-GTGAGCCCCAGCCTTCTCCAT-3') for the amplification of glycerol-3-phosphat dehydrogenase (GAPDH) mRNA.

The 3'-UTR and the 5'-UTR of vXCL1 were determined with the FirstChoice RLM-RACE Kit (Ambion) according to the manufacturer's instructions. *vxcl1* gene-specific primers *3'-UTR vXCL1* (5'-CACGAAACCATCTGCGTAAG-3') and *5'-UTR vXCL1* (5'-AGGAACCTGCGTGGGAATAACTG-3') were used for amplification of vXCL1-specific mRNA.

Generation of vXCL1-specific monoclonal antibody (mAb vXCL1.11). For overexpression, the complete coding region of vXCL1 was cloned into the BamHI site of vector pQE-30 (Qiagen) and transformed into *E. coli* host strain M15 [pREP4] (Qiagen). BALB/c mice were immunized subcutaneously with recombinant protein

(50 µg) in complete Freund´s adjuvant. Two weeks later, mice were boosted with the same protein in incomplete Freund´s adjuvant by injecting two-third volumes subcutaneously and one-third volume intraperitoneally (i.p.). After two weeks, sera of immunized mice were screened for antibody titer against the immunogen by ELISA. The best responders were additionally boosted i.p. with the immunogen dissolved in PBS. Three days later, spleen cells were collected and fused with SP2/0 myeloma cells at a ratio of 1:1 after lysis of red blood cells. Cells were seeded on 96-well tissue-culture plates in 20% RPMI 1640 medium containing hypoxanthine, aminopterine, and thymidine for hybridoma selection. Cultures were screened for monoclonal antibodies reactive against immunogens by ELISA. Positive mother wells were expanded and cloned. Mice used for immunization were bred and maintained under SPF conditions at the Laboratory Mouse Breeding and Engineering Centre (LAMRI) at the Faculty of Medicine, University of Rijeka. All experimental procedures were approved by the Ethics Committee of the University of Rijeka.

Other antibodies, flow cytometry and recombinant chemokines. Antibodies recognizing CD45RA (OX-33) and MHCII (OX-6) were from BD Pharmingen; anti-CD4 (W3/25) from AbDSerotec and anti-CD103 (OX62) from Biolegend. Mouse XCR1-specific monoclonal antibody (MARX10, (9), cross-reacting with rat XCR1) and goat serum directed against murine XCL1 (cross-reacting with vXCL1) were generated in the laboratory of R. Kroczek. Polyclonal rabbit anti-goat immunoglobulin-HRP and goat anti-mouse immunoglobulin-HRP were obtained from Dako. Flow cytometry data were acquired on an LSR II or FACSCalibur flow cytometer (BD Biosciences, San Jose, USA) using FACSDIVA or Cell Quest Pro software (BD Biosciences), respectively. Final examination and compensation of the

data were carried out using FlowJo software (Tree Star, Ashland, USA). vXCL1 and rat XCL1 containing an affinity tag at their respective carboxy termini were cloned into the expression vector pRmHa-3 (28) and expressed in stable drosophila SL-3 cell transfectants (L. Voss et al., manuscript in preparation).

Sandwich ELISA. 96-well Maxisorp microtiter plates (Nalgene Nunc, Roskilde, DK) were coated with 100 µl mAb vXCL1.11 (final concentration 1 µg/ml) diluted in coating buffer (0.1 M $NaHCO_3$, Na_2CO_3, pH 9.5) overnight at 4°C. Wells were washed five times with washing buffer (1x PBS containing 0.1 % (v/v) Tween-20) and blocked with blocking buffer (1% BSA (w/v) in washing buffer) for 2 h at RT. After five washes with washing buffer, 100 µl of test sample and serial dilutions of recombinant vXCL1 were applied per well and incubated for 2 h at RT. Unbound proteins were removed by rinsing five times with washing buffer, followed by 1 h incubation with cross-reactive goat serum directed against murine XCL1 (1:500 dilution) in blocking buffer at RT. Polyclonal anti-goat immunoglobulin-HRP was diluted in blocking buffer (final concentration 0.2 µg/ml) and added after rinsing five times with washing buffer for 1 h at RT. After ten additional washes, 50 µl of TMB Plus (KEM EN TEC, Taastrup, DK) was added to each well and incubated for five min in the dark. The reaction was stopped by adding 50 µl of 0.5 N H_2SO_4 and absorbance was determined at 450 nm using a Spectrafluor Plus (Tecan, San Jose, USA) microplate reader.

SDS-PAGE, immunoblotting and posttranslational modification analysis. To analyze N-glycosylation of vXCL1, lysates of MuHV8-infected REF (20 µg of total

protein of REF infected at MOI 10) were denatured for 10 min in 1x Glycoprotein Denaturing Buffer (NEB, Ipswich, USA) and then digested with 1 U PNGaseF (NEB) for 1.5 h at 37°C using 1x G7 Reaction Buffer (NEB) and 1% Nonidet P-40. The digested protein lysate was then mixed with 4x SDS loading buffer (0.3 M Tris, 12% SDS, 40% (v/v) glycerol, 0.3 M DTT, 0.02 bromophenole blue) and separated electrophoretically on a 15% Tris-Tricine SDS-gel using the prestained PageRuler™ ladder (Fermentas). Afterwards, the gel was blotted onto a Hybond™ ECL™ nitrocellulose membrane (GE Healthcare, Munich, GER) with 0.8 mA per cm^2 and stained with mAb vXCL1.11 using the ECL Western blotting reagents (GE Healthcare).

Mass-spectrometric peptide analysis. vXCL1 produced in insect cells was purified by heparin sepharose affinity chromatography. Peptides from the gel-purified protein were obtained by trypsin and endoproteinase Glu-C in-gel digestion as described previously (29) and peptide masses were analysed by matrix-assisted laser desorption ionization-time of flight mass spectrometry (MALDI-TOF-MS) using an Ultraflex-II TOF/TOF instrument (Bruker Daltonics, Bremen, GER) equipped with a 200 Hz solid-state Smart beam™ laser. The mass spectrometer was operated in the positive reflector mode; mass spectra were acquired over an m/z range from 600 to 4,000. α-cyano-4-hydroxycinnamic acid (CHCA) was used as the matrix and samples were spotted using the dried-droplet technique. MS/MS spectra of selected peptides were acquired in LIFT mode (30).

Cell isolation. Spleens of Lewis rats were cut into small pieces and digested with 500 µg/ml Collagenase D (Roche, Penzberg, GER) and 20 µg/ml DNase I (Roche) in RPMI 1640 containing 2% FCS (Pan Biotech GmbH, Regensburg, GER) for 25 min at 37°C and shaking at 200 rpm. After addition of 10 mM EDTA and incubation for five min at 37°C, cells were filtered through a 100 µm nylon sieve (BD Pharmingen) followed by NycoPrep density gradient (1.077 g/ml) for ten min at 1700 g and 4°C. The DC-enriched interphase was recovered and used for chemokine binding assays. For chemotaxis experiments, rat DC were enriched by magnetic cell sorting using CD103 microbeads according to the manufacturer's instructions (Miltenyi Biotec, Bergisch Gladbach, GER).

Chemotaxis assay. Migration of CD103-enriched splenocytes was analyzed in a migration assay as described elsewhere (31). In brief, $1 \cdot 10^5$-$5 \cdot 10^5$ CD103-enriched rat splenocytes were resuspended in chemotaxis medium (RPMI 1640, 1% BSA, 50 µM β-mercaptoethanol, 100 µg/ml penicillin/streptomycin) and placed in the upper chamber of a 24-well 6.5 mm transwell system (Corning, Salt Lake City, USA). The lower chamber was filled with chemotaxis medium containing the chemokine of interest, no chemokine as a control, or supernatant of infected REF. Cells were incubated for 2.5 h at 37°C and 5% CO_2. To examine the effect of Pertussis toxin (PTX) on cell migration, CD103-enriched splenocytes were treated with 100 ng/ml PTX (Sigma-Aldrich, Taufkirchen, GER) for 2 h at 37°C and 5% CO_2 and then washed twice with chemotaxis medium prior to migration analysis. Cells migrating into the lower chamber were analyzed by flow cytometry. T cells ($CD3^+$, $MHCII^-$), B cells ($CD45RA^+$, $MHCII^+$), $CD4^+$ DC ($MHCII^+$, $CD103^+$, $CD4^+$) and $CD4^-$ DC ($MHCII^+$, $CD103^+$, $CD4^-$) were identified by flow cytometry using the indicated markers.

Numbers of migrated cells and input cells were determined by counting cells over a time frame of 300 sec in a defined volume. Calculation of migrated cells was based on the number of input cells: number of migrated cells/ number of input cells x 100.

Results

MuHV8 encodes a C-chemokine homologue

Genome analysis of MuHV8 identified a 348 bp open reading frame (ORF) between viral genes *e155* and *e159* encoding a putative 115 amino-acid protein. Blast analysis at the protein level revealed 64 % identity (73 % homology) with the C-chemokine XCL1 of *Rattus norvegicus,* 58 % identity with mouse XCL1, and 46 % identity with human XCL1 (Fig. 1 A). Given the high degree of identity and homology to XCL1 and the conserved cysteines at positions 30 and 67, characteristic of C-chemokines, this putative protein was designated viral XCL1 (vXCL1). The highest divergence between vXCL1 and XCL1 was observed at the C-terminus, whereas the N-terminus and the core of the protein are conserved.

Rat, murine and human *xcl1* each contain three exons that are transcribed into a single mRNA (1, 32). In contrast, vXCL1 mRNA is unspliced. To investigate vXCL1 expression, mRNA of MuHV8-infected rat embryo fibroblasts (REF) was harvested and the three prime untranslated region (3'-UTR) and five prime untranslated region (5'-UTR) were determined by rapid amplification of cDNA ends (RACE). MuHV8 *vxcl1* encodes a transcript of 1689 bp consisting of a 99 bp 5'-UTR, a 348 bp ORF, and a 1,242 bp 3'-UTR (Fig. 1 B). Computational analysis detected four AU-rich elements (ARE), one Musashi binding element (MBE) in the 3'-UTR, and one MBE motif in the 5'-UTR of vXCL1 mRNA.

If vXCL1 were to be involved in immune evasion, precise timing of viral gene expression to bypass certain host immune responses can be expected; we therefore analyzed *vxcl1* expression kinetics. Semi-quantitative RT-PCR revealed that vXCL1 mRNA is already expressed two hours post infection and follows early kinetics (Fig. 1 C). To clarify if vXCL1 mRNA is produced immediate early or early, REF were treated with cycloheximide prior to infection. vXCL1 mRNA was not detected upon treatment with the protein synthesis inhibitor (Fig. 1 D), indicating that *vxcl1* is expressed early after infection in a protein-dependent fashion.

vXCL1 is a posttranslationally modified, secreted protein

To examine if and at what time postinfection vXCL1 is secreted, flow cytometry and sandwich enzyme-linked immunosorbent assays (ELISA) were carried out using a monoclonal antibody directed against vXCL1 (mAb vXCL1.11). As shown in Fig. 2 A, vXCL1 could be detected in infected cells by flow cytometry at 13 hours post infection and accumulated thereafter in the presence of Brefeldin A. A quantitative comparison of vXCL1 protein in lysates and supernatants of infected cells by ELISA revealed that vXCL1 is enriched over time in the supernatant of infected REF (Fig. 2 B). Only low amounts of viral protein were detected throughout the course of infection in cell lysate.

Chemokines are usually generated as precursor proteins containing an N-terminal signal peptide of approximately 20 residues (e.g., in human XCL1 (2)). Cleavage of the signal peptide yields the mature protein, which is secreted. In order to characterize the N-terminus of MuHV8 vXCL1 experimentally, the viral protein was expressed in insect cells and harvested from the supernatant by heparin affinity

chromatography. Following purification, recombinant vXCL1 was analyzed by peptide mass fingerprinting. MALDI mass spectrometric analysis of secreted vXCL1 detected isoleucine$_{20}$ (I_{20}) as the N-terminal amino acid, indicating that the precursor protein is cleaved between serine$_{19}$ (S_{19}) and isoleucine$_{20}$ (I_{20}), resulting in a 96-residue mature protein. Additionally, the analysis revealed the presence of another mature protein starting with isoleucine$_{22}$, although this form was less abundant. Fig. 2 C summarizes the structure of the two mature protein variants.

Chemokine glycosylation has been implicated in chemokine folding and stability, thereby influencing the interaction with the respective receptor (33). Glycosylation was found to modify human XCL1 in such a way that different molecular sizes become apparent in Western blot analysis (2). To clarify whether different posttranslationally modified versions of vXCL1 exist, lysates of REF infected with MuHV8 were analyzed by Western blot after digest with PNGaseF, an amidase cleaving N-linked oligosaccharides from asparagines. As shown in Fig. 2 D, PNGaseF treatment led to a size-shift of vXCL1, indicating the presence of N-linked sugars attached to the viral protein. These data were corroborated by mass spectrometrical analyses. PNGase F treatment resulted in a shift of the main peak from 12,778 to 10,701, indicating that vXCL1 is N-glycosylated (Fig. 2 E). The observed mass shift of 2,077 could best be explained by attachment of a $Man_3GlcNac_2Fuc$ moiety (m=1039) to each of the two potential N-glycosylation sites at N94 and N108. After removal of N-linked oligosaccharides the mass heterogeneity persisted, presumably due to heterogeneous O-glycosylation. In the spectrum of the N-deglycosylated sample the mass peak at 11,067 pointed to an additional HexNAc-Hex, compatible with a mucin-type O-glycan core structure. This peak could be eliminated by O-glycosidase, also known as endo-α-*N*-acetylgalactosaminidase, an

enzyme that preferentially catalyzes the removal of O-linked disaccharides from glycoproteins, while it does not attack more complex O-glycan structures. These findings suggest that vXCL1 is additionally O-glycosylated (Fig. 2 F).

vXCL1 is a chemoattractant for $CD4^-$ DC, but not for $CD4^+$ DC, T cells or B cells

Murine and human XCL1 exert their biological function by attracting XCR1-expressing DC. We therefore tested vXCL1 for chemotactic capacity on rat DC, which were defined as $CD103^+MHCII^+$ (34), and used rat XCL1 as a positive control. DC were obtained by collagenase digest of splenic tissue followed by NycoPrep density gradient centrifugation and magnetic sorting of $CD103^+$ cells. The enriched (60 %) DC population (composed of 36 % $CD4^+$ and 62 % $CD4^-$ DC; Fig. 3 A, input) was placed in the upper chamber of a transwell system. Only very low background migration was observed with $CD4^-$ DC and $CD4^+$ DC fractions (less than 5% of input cells) in the absence of rat XCL1 or vXCL1. With increasing concentrations of rat XCL1 and vXCL1, selective migration of $CD4^-$ DC occurred while $CD4^+$ DC essentially failed to migrate (Fig. 3 B and C). A concentration of either 100 ng/ml vXCL1 or rat XCL1 yielded the strongest migration of approximately 60 % of $CD4^-$ DC. vXCL1 and rat XCL1 did not induce migration of T or B cells (Fig. 3 D and E). These results demonstrate that vXCL1 is a bone fide chemokine selectively attracting $CD4^-$ DC, but not $CD4^+$ DC. Since chemokine receptors have been shown to signal *via* PTX-sensitive $G_{\alpha i}$ proteins (35), we investigated if the latter play a role in rat XCR1 signaling. DC were preincubated with 100 ng/ml PTX and analyzed for their ability to migrate towards vXCL1 and rat XCL1, respectively (Fig. 3 F). Migration of $CD4^-$ DC towards vXCL1 and rat XCL1 was blocked by PTX, indicating that XCR1 signaling involves $G_{\alpha i}$ protein.

MuHV8-infected cells secreting vXCL1 attract $CD4^-$ DC

Since recombinant vXCL1 induced migration of DC, it was expected that supernatant harvested from wild-type- but not *vxcl1*-deleted virus-infected cells would also result in DC migration. However, to rule out that differences in replication kinetics between wild-type and *vxcl1*-deleted MuHV-8 cause variations in DC migration, growth behavior of the viruses was analyzed and found to be similar (Fig. 4 A and B).

48 hours postinfection, supernatants of mock-infected, MuHV8 wild-type-infected and knockout virus (Δ*vxcl1*)-infected REF were analyzed in chemotaxis assays (Fig. 4 C). Supernatants of cells infected with MuHV8 Δ*vxcl1* failed to induce migration of $CD4^-$ DC above the background compared with supernatants obtained from mock-infected REF. In contrast, supernatants of MuHV8 wild-type-infected REF induced chemotaxis in more than 20 % of $CD4^-$ DC. None of the supernatants induced migration of T or B cells. Taken together, these data indicate that vXCL1 generated during infection selectively attracts $CD4^-$ DC.

Both vXCL1 and rat XCL1 bind to $XCR1^+CD4^-$ DC

In the mouse and the human, expression of XCR1 is restricted to a subset of DC (9, 31, 36). Since XCR1 is the only receptor for murine and human XCL1, we tested whether vXCL1 and rat XCL1 interact with rat XCR1. For these experiments we used mAb MARX10 which specifically recognizes murine XCR1 in a non-blocking fashion ((9)) and cross-reacts with rat XCR1 (Hartung et al., manuscript in preparation). $CD4^-$ and $CD4^+$ splenic DC were stained with MARX10 and co-stained with either rat XCL1 or vXCL1 (both tagged with a fluorochrome). As shown in Fig. 5, vXCL1 bound exclusively to $CD4^-$ DC expressing XCR1 (bold square). Neither $CD4^+$ DC, nor T cells or B cells exhibited any binding of the viral chemokine. Rat XCL1 was tested in parallel and demonstrated a very similar staining pattern.

Since rat XCL1 and vXCL1 are highly similar in their amino-acid sequence, induced chemotaxis and bound to the same cell subset, we tested whether they share the same receptor, XCR1. To address this question, enriched DC were incubated with rat XCL1-APC in the presence of increasing concentrations of unlabeled vXCL1, and *vice versa*. Fig. 6 A shows that binding of rat XCL1-APC to $CD4^-$ DC was effectively competed by unlabeled vXCL1. Analogous results were obtained when DC were incubated with vXCL1-APC in the presence of unlabeled rat XCL1 (Fig. 6 B). These findings indicate that both chemokines bind to the same receptor on $CD4^-$ DC.

Discussion

CMV encodes several proteins that interfere with the chemokine network of the host. These proteins include molecules which act as chemokines (21), as chemokine-binding proteins (37), or as chemokine receptors (38, 39). In our study we identified and characterized a C-chemokine encoded by MuHV8, vXCL1, to our knowledge the first reported viral C-chemokine. We could not identify sequence homologues in any other virus by database screening.

Blast analysis of the vXCL1 amino-acid sequence revealed high similarity to the only known C-chemokine expressed in rat, mouse and human, XCL1. XCL1 in various species and vXCL1 have a similar length of 114-115 amino acids in their immature form. Both mouse and rat *xcl1* have three coding exons. Rat *xcl1* (GenBank Gene ID: 171371) has a size of 3.44 kbp with a transcript length of 345 bp, mouse *xcl1* (GenBank Gene ID: 16963, (40)) has a size of 3.88 kbp with a transcript of 523 bp. The *vxcl1* transcript of 1.6 kbp (including a 1.2 kbp 3'-UTR) originates from a continuous viral gene segment and contains one MBE motif and various AU-rich elements. In contrast to *vxcl1*, the MuHV8-encoded CC-chemokine *eck-2* was acquired as an unspliced transcript with intron/exon boundaries similar to *mck-2* in mCMV (24). Possibly, acquisition of unspliced transcripts enables different levels of regulation of the CC-chemokines whereas this might not occur in the case of *vxcl1*.

Expression of immunomodulatory CMV genes is precisely timed to compromise cellular defense strategies (41). We therefore carefully analyzed both vXCL1 mRNA and protein expression kinetics. Semi-quantitative RT-PCR revealed that vXCL1 mRNA is expressed two hours post infection and therefore follows early kinetics. In contrast to these results, intracellular vXCL1 protein could only be detected 13 hours after infection. Since the vXCL1 transcript contains various RNA-binding protein

405 motifs, it is conceivable that vXCL1 mRNA translation is inhibited early during
406 infection through the interaction with RNA-binding proteins. Moreover, vXCL1 mRNA
407 contains more AU-rich elements and also other potential binding sites for proteins
408 and microRNAs than host rat XCR1. These sites might influence translation of vXCL1
409 mRNA and could serve as an explanation for the discrepancy between mRNA
410 production and the onset of protein expression.

411 Correct cleavage of the signal peptide in the conversion of an immature chemokine
412 into its mature form is critical for receptor binding and function (42). Since vXCL1 was
413 secreted and enriched in the supernatant of infected REF, we performed mass
414 spectrometric analysis to determine the N-terminus of the mature protein. The
415 supernatants contained two variants of vXCL1: an abundant mature protein spanning
416 from isoleucine$_{20}$ to glycine$_{115}$ and a less abundant truncated protein ranging from
417 isoleucine$_{22}$ to glycine$_{115}$. In addition, vXCL1 was shown to contain N-linked sugars
418 since PNGaseF treatment resulted in a size shift as detected by Western blot and
419 mass spectrometric analyses. The vXCL1 amino-acid sequences possess two N-
420 glycosylation motifs at which N-glycosylation could take place: Asn$_{94}$-Thr$_{95}$-Thr$_{96}$ and
421 Asn$_{108}$-Glu$_{109}$-Thr$_{110}$. The N-linked-sugars of vXCL1 might improve interaction with
422 the chemokine receptor, increase the stability and thus the biological activity of the
423 chemokine, or might help to mask antigenic sites of the viral molecule. Interestingly,
424 human and murine XCL1 presumably carry O-linked sugars at their respective C-
425 terminus (2, 43). NetOGlyc analysis predicted several potential O-glycosylation sites
426 for vXCL1 at the C-terminus, and mass spectrometric analysis confirmed that vXCL1
427 possesses an O-linked sugar.

428 Murine and human XCL1 have been shown to act as chemoattractants on cross-
429 presenting DC (9, 31, 36) while there are no data available in the rat. We therefore

compared vXCL1 and rat XCL1 in their ability to induce migration of $CD4^-$ DC, $CD4^+$ DC, B cells, and T cells. Our data demonstrate that only $CD4^-$ DC migrate in the presence of either the host or viral chemokine. Similar findings were obtained when supernatants of infected REF were used in chemotaxis assays: only supernatants of MuHV8-infected REF but not those of Δ*vxcl1*-infected cells attracted $CD4^-$ DC. A revertant virus was not employed in these assays because complete genome sequencing of the MuHV8 Δ*vxcl1* knockout virus and comparison with wild-type MuHV8 showed only the desired sequence divergence in the v*xcl1* region but not elsewhere in the genome. Rat $CD4^-$ DC are thought to be the equivalent of murine $CD8^+$ DC (44, 45) since they both produce high amounts of interleukin 12 (45), efficiently phagocytose apoptotic cells, and are located in the red pulp and T cell area of the spleen (46). The findings that both rat XCL1 and vXCL1 selectively induce migration of only $CD4^-$ DC further support the concept that these DC are the equivalents of human (31, 47) and murine cross-presenting DC (9).

The G protein-coupled receptor XCR1 was shown to be expressed only on cross-presenting DC in mice (9) and was identified as the only interaction partner of XCL1 in the human and murine system. Thus, XCR1 is the most prominent candidate as a vXCL1 and rat XCL1 interaction partner. The monoclonal antibody MARX10 directed against mouse XCR1 (9) cross-reacts with rat XCR1 and therefore served as a valuable tool to analyze the correlation between chemokine binding and receptor expression. Approximately 80 % of rat $CD4^-$ DC expressed XCR1, which correlates with the murine system where 70-85 % of spleen-derived $CD8^+$ DC were shown to express XCR1 (9, 36). Flow cytometry studies revealed that vXCL1 and rat XCL1 bound selectively to $CD4^-$, XCR1-expressing DC. Chemokine binding to $CD4^+$ DC was not observed which is in accordance with our chemotaxis data.

Upon ligand binding, intracellular G proteins are dissociated into GTP-bound subunits and a signal cascade that results in cell migration is initiated. Since little is known about rat XCR1-mediated signaling, we addressed the question if vXCL1- or rat XCL1-mediated migration can be inhibited by treatment with PTX, an agent that modifies $G\alpha_i$ proteins, and if this would prevent $G\alpha_i$ protein interaction with XCR1 and abolish DC migration. Indeed, preincubation with PTX inhibited $CD4^-$ DC migration, suggesting that rat XCR1 is linked with a $G\alpha_i$ protein.

Since both rat XCL1 and vXCL1 bound to $XCR1^+CD4^-$ DC, it was likely that both chemokines share the interaction partner. However, it was not clear if XCR1 is the only interaction partner or if another receptor co-expressed with XCR1 is targeted. To address this question, we examined binding of rat XCL1-APC to rat DC subsets in the presence of different concentrations of unlabeled vXCL1, and *vice versa*. Competitive binding studies revealed that binding of APC-labeled rat XCL1 was abolished in the presence of unlabeled vXCL1 and *vice versa*, implying that vXCL1 binds to the same surface molecule, i.e., XCR1.

The data presented here show that vXCL1 i) has chemokine-like properties, ii) binds to and attracts $CD4^-$ rat DC that express XCR1, and iii) functionally resembles rat XCL1. At first glance, the attraction of $XCR1^+$ DC seems rather unfavorable for the virus. In mice and humans, XCR1-expressing DC are capable of antigen cross-presentation and thus possess a key role in controlling viruses (10, 11). In the mouse model, $CD8^+$ cross-presenting DC could be infected with MCMV at low percentage (48, 49). Infection of DC was shown to be accompanied by reduced surface expression of MHC class I and II molecules (50-52), altered cytokine and chemokine receptor expression (53), and down-regulation of molecules required for T and NK cell proliferation (48, 50, 52). Since DC are important for regulating and controlling T

and NK cell responses (54, 55) and the latter play a major role in controlling CMV infection (56-60), MuHV8 might infect and functionally paralyze this DC subset by vXCL1 attraction in order to impair antiviral responses. Further, immature DC have been shown to be an important reservoir of latent CMV from which reactivation can occur (61, 62), but it remains to be determined if vXCL1 has a role in the establishment of a latent infection.

Alternatively, it is possible that cross-presenting DC regulate T cell activation and cytotoxicity without being infected and that vXCL1 functions analogous to the MCMV-encoded CC-chemokine MCK-2. MCK-2 attracts inflammatory monocytes to the site of infection where they compromise virus-specific $CD8^+$ T cells and thus contributes to viral persistence (26). Possibly, vXCL1 attracts $XCR1^+$ DC to the site of infection and locally disturbs cooperation with $CD8^+$ T cells, thereby compromising the adaptive immune response. However, it remains to be shown if the attracted $XCR1^+$ DC subset is able to cross-present antigen. Eventually, the influence of MuHV8 on this potentially cross-presenting DC subset and possible vXCL1-interference with the host immune system will have to be evaluated in *in vivo* studies.

So far, all CMV-encoded chemokines were classified as either CXC- or CC-chemokines and have been shown to attract neutrophils (17), monocytes (25), macrophages (63), and $CD4^+$ T cells (20). vXCL1 is the first reported CMV-encoded C-chemokine that targets $XCR1^+CD4^-$DC. This might imply an important physiological function since also Kaposi sarcoma-associated herpesvirus (KSHV) has been shown to encode two chemokines, vCCL2 and vCCL3, which likewise target XCR1 at different time points during infection (64, 65). The observation that both MuHV8 and

KSHV exploit XCR1 with different virally-encoded chemokines suggests a substantial importance of this receptor in the defense against herpesviruses.

Since MuHV8 is so far the only known virus to encode an XCL1 homologue, the MuHV8-rat model appears particularly useful in analyzing the biological function of vXCL1 and its interference with the endogenous XCL1 molecule. Thus, this model offers a unique opportunity to study the involvement of XCL1 in antiviral defenses and might be promising to provide clues for novel antiviral strategies.

Acknowledgments

We would like to thank Marina Babić as well as Brigitte Dorner and Martin Dorner for expert help. S.V. is supported by the Deutsche Forschungsgemeinschaft (VO 774/7).

References

1. **Yoshida T, Imai T, Takagi S, Nishimura M, Ishikawa I, Yaoi T, Yoshie O.** 1996. Structure and expression of two highly related genes encoding SCM-1/human lymphotactin. FEBS Lett. **395:**82-88.
2. **Dorner B, Müller S, Entschladen F, Schröder JM, Franke P, Kraft R, Friedl P, Clark-Lewis I, Kroczek RA.** 1997. Purification, structural analysis, and function of natural ATAC, a cytokine secreted by $CD8^{(+)}$ T cells. J. Biol. Chem. **272:**8817-8823.
3. **Dorner BG, Smith HR, French AR, Kim S, Poursine-Laurent J, Beckman DL, Pingel JT, Kroczek RA, Yokoyama WM.** 2004. Coordinate expression of cytokines and chemokines by NK cells during murine cytomegalovirus infection. J. Immunol. **172:**3119-3131.

4. **Dorner BG, Scheffold A, Rolph MS, Hüser MB, Kaufmann SH, Radbruch A, Flesch IE, Kroczek RA.** 2002. MIP-1alpha, MIP-1beta, RANTES, and ATAC/lymphotactin function together with IFN-gamma as type 1 cytokines. Proc. Natl. Acad. Sci. U. S. A. **99:**6181-6186.

5. **Heiber M, Docherty JM, Shah G, Nguyen T, Cheng R, Heng HH, Marchese A, Tsui LC, Shi X, George SR, O'Dowd BF.** 1995. Isolation of three novel human genes encoding G protein-coupled receptors. DNA Cell. Biol. **14:**25-35.

6. **Yoshida T, Imai T, Kakizaki M, Nishimura M, Takagi S, Yoshie O.** 1998. Identification of single C motif-1/lymphotactin receptor XCR1. J. Biol. Chem. **273:**16551-16554.

7. **Pooley JL, Heath WR, Shortman K.** 2001. Cutting edge: intravenous soluble antigen is presented to CD4 T cells by $CD8^-$ dendritic cells, but cross-presented to CD8 T cells by $CD8^+$ dendritic cells. J. Immunol. **166:**5327-5330.

8. **den Haan JM, Lehar SM, Bevan MJ.** 2000. $CD8^{(+)}$ but not $CD8^{(-)}$ dendritic cells cross-prime cytotoxic T cells in vivo. J. Exp. Med. **192:**1685-1696.

9. **Bachem A, Hartung E, Güttler S, Mora A, Zhou X, Hegemann A, Plantinga M, Mazzini E, Stoitzner P, Gurka S, Henn V, Mages HW, Kroczek RA.** 2012. Expression of XCR1 characterizes the Batf3-dependent lineage of dendritic cells capable of antigen cross-presentation. Front. Immunol. **3:**214.

10. **Rock KL, Shen L.** 2005. Cross-presentation: underlying mechanisms and role in immune surveillance. Immunol. Rev. **207:**166-183.

11. **Shortman K, Heath WR.** 2010. The $CD8^+$ dendritic cell subset. Immunol. Rev. **234:**18-31.

12. **Kroczek RA, Henn V.** 2012. The role of XCR1 and its ligand XCL1 in antigen cross-presentation by murine and human dendritic cells. Front. Immunol. **3:**14.

13. **Mocarski ES, Shenk T, Pass RF.** 2007. Cytomegaloviruses., p. 2703-2772. *In* Knipe DM, Howley PM (ed.), Fields Virology 5ed, vol. 1 Lippincott Williams and Wilkins, Philadelphia, PA.

14. **Beisser PS, Lavreysen H, Bruggeman CA, Vink C.** 2008. Chemokines and chemokine receptors encoded by cytomegaloviruses. Curr. Top. Microbiol. Immunol. **325:**221-242.

15. **Akter P, Cunningham C, McSharry BP, Dolan A, Addison C, Dargan DJ, Hassan-Walker AF, Emery VC, Griffiths PD, Wilkinson GW, Davison AJ.** 2003. Two novel spliced genes in human cytomegalovirus. J. Gen. Virol. **84:**1117-1122.

16. **Penfold ME, Dairaghi DJ, Duke GM, Saederup N, Mocarski ES, Kemble GW, Schall TJ.** 1999. Cytomegalovirus encodes a potent alpha chemokine. Proc. Natl. Acad. Sci. U. S. A. **96:**9839-9844.

17. **Lüttichau HR.** 2010. The cytomegalovirus UL146 gene product vCXCL1 targets both CXCR1 and CXCR2 as an agonist. J. Biol. Chem. **285:**9137-9146.

18. **Straschewski S, Patrone M, Walther P, Gallina A, Mertens T, Frascaroli G.** 2011. Protein pUL128 of human cytomegalovirus is necessary for monocyte infection and blocking of migration. J. Virol. **85:**5150-5158.

19. **Gao H, Tao R, Zheng Q, Xu J, Shang S.** 2013. Recombinant HCMV UL128 expression and functional identification of PBMC-attracting activity in vitro. Arch. Virol. **158:**173-177.

20. **Vomaske J, Denton M, Kreklywich C, Andoh T, Osborn JM, Chen D, Messaoudi I, Orloff SL, Streblow DN.** 2012. Cytomegalovirus CC chemokine promotes immune cell migration. J. Virol. **86:**11833-11844.

21. **van Cleef KW, Smit MJ, Bruggeman CA, Vink C.** 2006. Cytomegalovirus-encoded homologs of G protein-coupled receptors and chemokines. J. Clin. Virol. **35:**343-348.

22. **Vink C, Beuken E, Bruggeman CA.** 2000. Complete DNA sequence of the rat cytomegalovirus genome. J. Virol. **74:**7656-7665.

23. **Saederup N, Aguirre SA, Sparer TE, Bouley DM, Mocarski ES.** 2001. Murine cytomegalovirus CC chemokine homolog MCK-2 (m131-129) is a determinant of dissemination that increases inflammation at initial sites of infection. J. Virol. **75:**9966-9976.

24. **Voigt S, Sandford GR, Hayward GS, Burns WH.** 2005. The English strain of rat cytomegalovirus (CMV) contains a novel captured CD200 (vOX2) gene and a spliced CC chemokine upstream from the major immediate-early region: further evidence for a separate evolutionary lineage from that of rat CMV Maastricht. J. Gen. Virol. **86:**263-274.

25. **Noda S, Aguirre SA, Bitmansour A, Brown JM, Sparer TE, Huang J, Mocarski ES.** 2006. Cytomegalovirus MCK-2 controls mobilization and recruitment of myeloid progenitor cells to facilitate dissemination. Blood **107:**30-38.

26. **Daley-Bauer LP, Wynn GM, Mocarski ES.** 2012. Cytomegalovirus impairs antiviral $CD8^+$ T cell immunity by recruiting inflammatory monocytes. Immunity **37:**122-133.

27. **Ettinger J, Geyer H, Nitsche A, Zimmermann A, Brune W, Sandford GR, Hayward GS, Voigt S.** 2012. Complete genome sequence of the english isolate of rat cytomegalovirus (Murid herpesvirus 8). J. Virol. **86:**13838.

28. **Wallny HJ.** 1997. Production of soluble MHC class II molecules in Drosophila melanogaster Schneider cells Immunol. Methods Manual **1:**51-59.

29. **Shevchenko A, Wilm M, Vorm O, Mann M.** 1996. Mass spectrometric sequencing of proteins silver-stained polyacrylamide gels. Anal. Chem. **68:**850-858.

30. **Suckau D, Resemann A, Schuerenberg M, Hufnagel P, Franzen J, Holle A.** 2003. A novel MALDI LIFT-TOF/TOF mass spectrometer for proteomics. Anal. Bioanal. Chem. **376:**952-965.

31. **Bachem A, Güttler S, Hartung E, Ebstein F, Schaefer M, Tannert A, Salama A, Movassaghi K, Opitz C, Mages HW, Henn V, Kloetzel PM, Gurka S, Kroczek RA.** 2010. Superior antigen cross-presentation and XCR1 expression define human $CD11c^{+}CD141^{+}$ cells as homologues of mouse $CD8^{+}$ dendritic cells. J. Exp. Med. **207:**1273-1281.

32. **Hautamaa D, Merica R, Chen Z, Jenkins MK.** 1997. Murine lymphotactin: gene structure, post-translational modification and inhibition of expression by CD28 costimulation. Cytokine **9:**375-382.

33. **Mortier A, Van Damme J, Proost P.** 2008. Regulation of chemokine activity by posttranslational modification. Pharmacol. Ther. **120:**197-217.

34. **Voisine C, Hubert FX, Trinite B, Heslan M, Josien R.** 2002. Two phenotypically distinct subsets of spleen dendritic cells in rats exhibit different cytokine production and T cell stimulatory activity. J. Immunol. **169:**2284-2291.

35. **Thelen M.** 2001. Dancing to the tune of chemokines. Nat. Immunol. **2:**129-134.

36. **Dorner BG, Dorner MB, Zhou X, Opitz C, Mora A, Güttler S, Hutloff A, Mages HW, Ranke K, Schaefer M, Jack RS, Henn V, Kroczek RA.** 2009. Selective expression of the chemokine receptor XCR1 on cross-presenting dendritic cells determines cooperation with $CD8^{+}$ T cells. Immunity **31:**823-833.

37. **Wang D, Bresnahan W, Shenk T.** 2004. Human cytomegalovirus encodes a highly specific RANTES decoy receptor. Proc. Natl. Acad. Sci. U. S. A. **101:**16642-16647.

38. **Alcami A, Saraiva M.** 2009. Chemokine binding proteins encoded by pathogens. Adv. Exp. Med. Biol. **666:**167-179.

39. **Murphy PM.** 2001. Viral exploitation and subversion of the immune system through chemokine mimicry. Nat. Immunol. **2:**116-122.

40. **Kelner GS, Kennedy J, Bacon KB, Kleyensteuber S, Largaespada DA, Jenkins NA, Copeland NG, Bazan JF, Moore KW, Schall TJ, Zlotnik A.** 1994. Lymphotactin: a cytokine that represents a new class of chemokine. Science **266:**1395-1399.

41. **Loewendorf A, Benedict CA.** 2010. Modulation of host innate and adaptive immune defenses by cytomegalovirus: timing is everything. J. Intern. Med. **267:**483-501.

42. **Allen SJ, Crown SE, Handel TM.** 2007. Chemokine: receptor structure, interactions, and antagonism. Ann. Rev. Immunol. **25:**787-820.

43. **Dorner BG, Steinbach S, Hüser MB, Kroczek RA, Scheffold A.** 2003. Single-cell analysis of the murine chemokines MIP-1alpha, MIP-1beta, RANTES and ATAC/lymphotactin by flow cytometry. J. Immunol. Meth. **274:**83-91.

44. **Hubert FX, Voisine C, Louvet C, Heslan JM, Ouabed A, Heslan M, Josien R.** 2006. Differential pattern recognition receptor expression but stereotyped responsiveness in rat spleen dendritic cell subsets. J. Immunol. **177:**1007-1016.

45. **Yrlid U, Macpherson G.** 2003. Phenotype and function of rat dendritic cell subsets. APMIS **111:**756-765.

46. **Trinite B, Chauvin C, Peche H, Voisine C, Heslan M, Josien R.** 2005. Immature $CD4^-$ $CD103^+$ rat dendritic cells induce rapid caspase-independent apoptosis-like cell death in various tumor and nontumor cells and phagocytose their victims. J. Immunol. **175:**2408-2417.

47. **Crozat K, Guiton R, Contreras V, Feuillet V, Dutertre CA, Ventre E, Vu Manh TP, Baranek T, Storset AK, Marvel J, Boudinot P, Hosmalin A, Schwartz-Cornil I, Dalod M.** 2010. The XC chemokine receptor 1 is a conserved selective marker of mammalian cells homologous to mouse $CD8alpha^+$ dendritic cells. J. Exp. Med. **207:**1283-1292.

48. **Andrews DM, Scalzo AA, Yokoyama WM, Smyth MJ, Degli-Esposti MA.** 2003. Functional interactions between dendritic cells and NK cells during viral infection. Nat. Immunol. **4:**175-181.

49. **Dalod M, Hamilton T, Salomon R, Salazar-Mather TP, Henry SC, Hamilton JD, Biron CA.** 2003. Dendritic cell responses to early murine cytomegalovirus infection: subset functional specialization and differential regulation by interferon alpha/beta. J. Exp. Med. **197:**885-898.

50. **Grigoleit U, Riegler S, Einsele H, Laib Sampaio K, Jahn G, Hebart H, Brossart P, Frank F, Sinzger C.** 2002. Human cytomegalovirus induces a direct inhibitory effect on antigen presentation by monocyte-derived immature dendritic cells. Br. J. Haematol. **119:**189-198.

51. **Kessler T, Reich M, Jahn G, Tolosa E, Beck A, Kalbacher H, Overkleeft H, Schempp S, Driessen C.** 2008. Human cytomegalovirus infection interferes with major histocompatibility complex type II maturation and endocytic proteases in dendritic cells at multiple levels. J. Gen. Virol. **89:**2427-2436.

52. **Andrews DM, Andoniou CE, Granucci F, Ricciardi-Castagnoli P, Degli-Esposti MA.** 2001. Infection of dendritic cells by murine cytomegalovirus induces functional paralysis. Nat. Immunol. **2:**1077-1084.

53. **Varani S, Frascaroli G, Homman-Loudiyi M, Feld S, Landini MP, Soderberg-Naucler C.** 2005. Human cytomegalovirus inhibits the migration of immature dendritic cells by down-regulating cell-surface CCR1 and CCR5. J. Leukoc. Biol. **77:**219-228.

54. **Steinman RM, Hawiger D, Liu K, Bonifaz L, Bonnyay D, Mahnke K, Iyoda T, Ravetch J, Dhodapkar M, Inaba K, Nussenzweig M.** 2003. Dendritic cell function in vivo during the steady state: a role in peripheral tolerance. Ann. N. Y. Acad. Sci. **987:**15-25.

55. **Wehner R, Dietze K, Bachmann M, Schmitz M.** 2011. The bidirectional crosstalk between human dendritic cells and natural killer cells. J. Innate Immun. **3:**258-263.

56. **Scalzo AA, Corbett AJ, Rawlinson WD, Scott GM, Degli-Esposti MA.** 2007. The interplay between host and viral factors in shaping the outcome of cytomegalovirus infection. Immunol. Cell Biol. **85:**46-54.

57. **Biron CA, Byron KS, Sullivan JL.** 1989. Severe herpesvirus infections in an adolescent without natural killer cells. N. Engl. J. Med. **320:**1731-1735.

58. **Reddehase MJ, Weiland F, Münch K, Jonjic S, Lüske A, Koszinowski UH.** 1985. Interstitial murine cytomegalovirus pneumonia after irradiation: characterization of cells that limit viral replication during established infection of the lungs. J. Virol. **55:**264-273.

59. **Riddell SR, Watanabe KS, Goodrich JM, Li CR, Agha ME, Greenberg PD.** 1992. Restoration of viral immunity in immunodeficient humans by the adoptive transfer of T cell clones. Science **257:**238-241.

60. **Kapp M, Tan SM, Einsele H, Grigoleit G.** 2007. Adoptive immunotherapy of HCMV infection. Cytotherapy **9:**699-711.

61. **Sinclair J.** 2008. Human cytomegalovirus: Latency and reactivation in the myeloid lineage. J. Clin. Virol. **41:**180-185.

62. **Sinclair J, Sissons P.** 2006. Latency and reactivation of human cytomegalovirus. J. Gen. Virol. **87:**1763-1779.

63. **Kaptein SJ, van Cleef KW, Gruijthuijsen YK, Beuken EV, van Buggenhout L, Beisser PS, Stassen FR, Bruggeman CA, Vink C.** 2004. The r131 gene of rat cytomegalovirus encodes a proinflammatory CC chemokine homolog which is essential for the production of infectious virus in the salivary glands. Virus Genes **29:**43-61.

64. **Lüttichau HR, Lewis IC, Gerstoft J, Schwartz TW.** 2001. The herpesvirus 8-encoded chemokine vMIP-II, but not the poxvirus-encoded chemokine MC148, inhibits the CCR10 receptor. Eur. J. Immunol. **31:**1217-1220.

65. **Lüttichau HR, Johnsen AH, Jurlander J, Rosenkilde MM, Schwartz TW.** 2007. Kaposi sarcoma-associated herpes virus targets the lymphotactin receptor with both a broad spectrum antagonist vCCL2 and a highly selective and potent agonist vCCL3. J. Biol. Chem. **282:**17794-17805.

730 **Legends to figures**

731

732 **Figure 1. Characterization of MuHV8-encoded C-chemokine vXCL1. (A)** Muscle
733 alignment (Geneious version 5.5.7, http://www.geneious.com) of amino-acid
734 sequences of vXCL1 and rat, mouse, and human XCL1. Identical amino acids are
735 indicated by black background, similar amino acids by gray background, and a lack of
736 similarity by white background. Cysteine positions characteristic of C-chemokines are
737 indicated by asterisks. Numbering refers to the amino-acid positions of the viral
738 chemokine. Accession numbers for the sequences depicted are JX867617.1 (vXCL1,
739 MuHV8); NP_599188 (rXCL1, *Rattus norvegicus* XCL1); NP_032536 (mXCL1, *Mus*
740 *musculus* XCL1); NP_002986 (hXCL1, *Homo sapiens* XCL1). **(B)** Analysis of vXCL1
741 mRNA. Total RNA from MuHV8-infected REF was isolated 24 hpi and 3'- and 5'-UTR
742 were determined. A Musashi binding element (MBE) was detected using UTRScan,
743 an AU-rich element (ARE) was identified by scanning for an AUUUA-element with
744 CloneManager (Sci-Ed software, Cary, USA). **(C)** Time course of MuHV8 vXCL1
745 expression. Total RNA from wild-type MuHV8 and MuHV8 Δ*vxcl1*-infected cells was
746 harvested at indicated time points, reverse-transcribed with oligo (dT) primers, and
747 amplified with *vxcl1*-specific primers. **(D)** Cycloheximide (CHX) was used to
748 discriminate between immediate early and early gene expression. MuHV8 Δ*vxcl1*
749 was included as a negative control. The experiment was carried out at least twice
750 with similar results. C-myc and GAPDH served as controls. hpi, hours post infection;
751 RT, reverse transcriptase.

752

Figure 2. Analysis of vXCL1 protein expression and posttranslational modification. (A) Protein expression kinetics of vXCL1. MuHV8-infected REF were treated 3 h before harvest with Brefeldin A, harvested at indicated time points and analyzed by flow cytometry using mAb vXCL1.11 which specifically recognizes vXCL1 (gray line). REF infected with MuHV8 Δ*vxcl1* served as a control (black line). **(B)** Secretion of vXCL1. Supernatants (gray bars) and lysates (black bars) of infected REF were collected at indicated time points and tested for the presence of vXCL1 by sandwich ELISA. Values were normalized by subtracting the mean of the value obtained with MuHV8 Δ*vxcl1*-infected cells. Results shown are from two independent experiments. Error bars represent means ± standard deviation (SD). **(C)** Schematic overview of the precursor protein and the two variants of mature vXCL1 determined by mass spectrometric analysis. **(D)** N-glycosylation variants of vXCL1. Lysates of MuHV8-infected REF were digested for 1.5 h in the presence or absence of PNGaseF and separated electrophoretically on a 15% Tris-Tricine polyacrylamide gel, followed by blotting and detection using mAb vXCL1.11. **(E)** Mass spectrometric analysis of vXCL1 N-glycosylation. PNGase F treatment resulted in a main peak shift from 12,778 to 10,701, the expected mass of the vXCL1 protein. **(F)** Mass spectrometric analysis of vXCL1 O-glycosylation. The mass peak at 11,067 in the N-deglycosylated sample (top panel) could be eliminated by O-Glycosidase (bottom panel).

Figure 3. Analysis of vXCL1 chemotactic activity. (A) Magnetically sorted splenic DC were tested for migration towards different concentrations of vXCL1 and rat XCL1 (10-1000 ng/ml) in a transwell assay. DC subpopulations were defined based on expression of CD103 and CD4. The dot plots represent the numbers of $CD4^-$ DC and $CD4^+$ DC which have migrated into the lower chamber. **(B)** and **(C)** Proportion of

778 migrated $CD4^-$ and $CD4^+$ DC in response to different concentrations of rat XCL1 and
779 vXCL1. **(D)** and **(E)** Proportion of migrated T and B cells towards rat XCL1 and
780 vXCL1. **(F)** Pertussis toxin (PTX) blocks migration of $CD4^-$ DC towards rat XCL1 and
781 vXCL1. No migration is detected in the absence of chemokine (control). All
782 experiments were performed twice. Error bars represent means ± SEM.

783

784 **Figure 4. vXCL1 is dispensable for viral growth in cell culture and attracts $CD4^-$**
785 **DC.** Growth of wild-type MuHV8 and MuHV8 Δ*vxcl1*. REF were infected at **(A)** MOI 5
786 and **(B)** 0.05, respectively, and titers were determined at the indicated time points by
787 plaque assay. Results were obtained from three independent experiments. **(C)** The
788 ability of vXCL1 to induce chemotaxis of different rat cell subsets was analyzed with
789 supernatants of mock-infected, wild-type MuHV8, and MuHV8 Δ*vxcl1*-infected REF.
790 Results were obtained from two independent experiments. Error bars represent
791 means ± SD.

792

793 **Figure 5. Analysis of rat XCL1 and vXCL1 binding to XCR1.** Splenic rat DC
794 ($MHCII^+CD103^+CD3^-CD45RA^-$) were gated into $CD4^+$ (upper panel) and $CD4^-$ (lower
795 panel) DC subsets and analyzed for binding of XCL1, vXCL1, and mAb MARX10.
796 Both rat XCL1 and vXCL1 selectively bound to DC expressing XCR1 (bold frames),
797 inset numbers give the proportion of double-positive cells. One representative
798 experiment out of three is shown.

799

800 **Figure 6. Competitive binding of vXCL1 and rat XCL1 to rat $CD4^-$ DC.** NycoPrep
801 gradient-enriched rat DC were incubated with **(A)** 400 ng/ml rat XCL1-APC in the

802 presence of different concentrations of unlabeled vXCL1, or with **(B)** 400 ng/ml
803 vXCL1-APC in the presence of different concentrations of unlabeled rat XCL1,
804 washed, and analyzed for binding of the respective fluorophore-tagged chemokine to
805 rat DC ($CD103^{+}MHCII^{+}$). In both instances, binding of the labeled chemokine was
806 effectively competed by the unlabeled chemokine on $CD4^{-}$ DC (lower right
807 quadrants). One representative experiment out of two is shown.

808

809

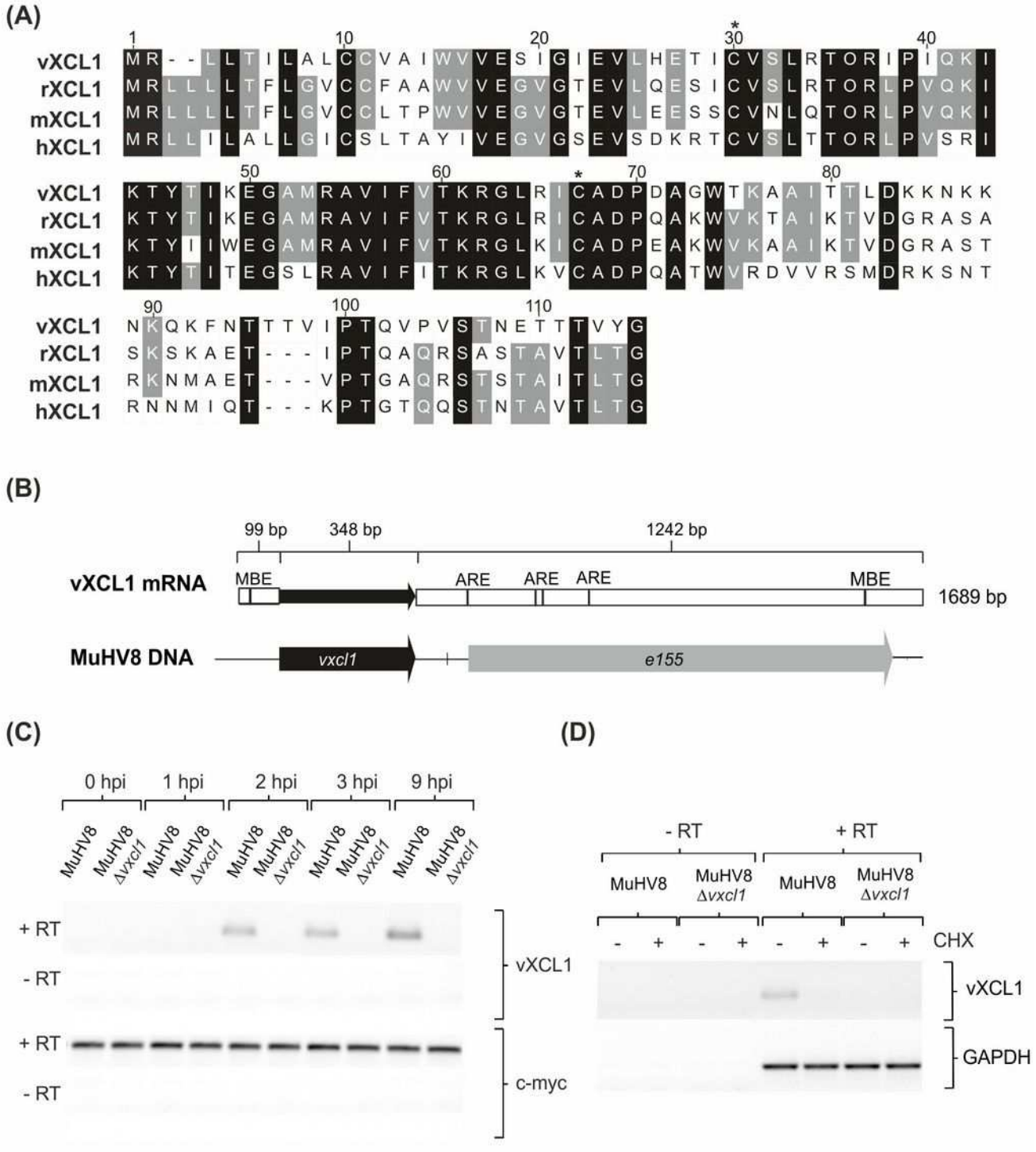
(A)
vXCL1
rXCL1
mXCL1
hXCL1
(B)
99 bp
348 bp
1242 bp
vXCL1 mRNA
MBE
ARE
ARE
ARE
MBE
1689 bp
MuHV8 DNA
vxcl1
e155
(C)
0 hpi
1 hpi
2 hpi
3 hpi
9 hpi
MuHV8
MuHV8 Δvxcl1
+ RT
- RT
vXCL1
c-myc
(D)
- RT
+ RT
MuHV8
MuHV8 Δvxcl1
CHX
vXCL1
GAPDH

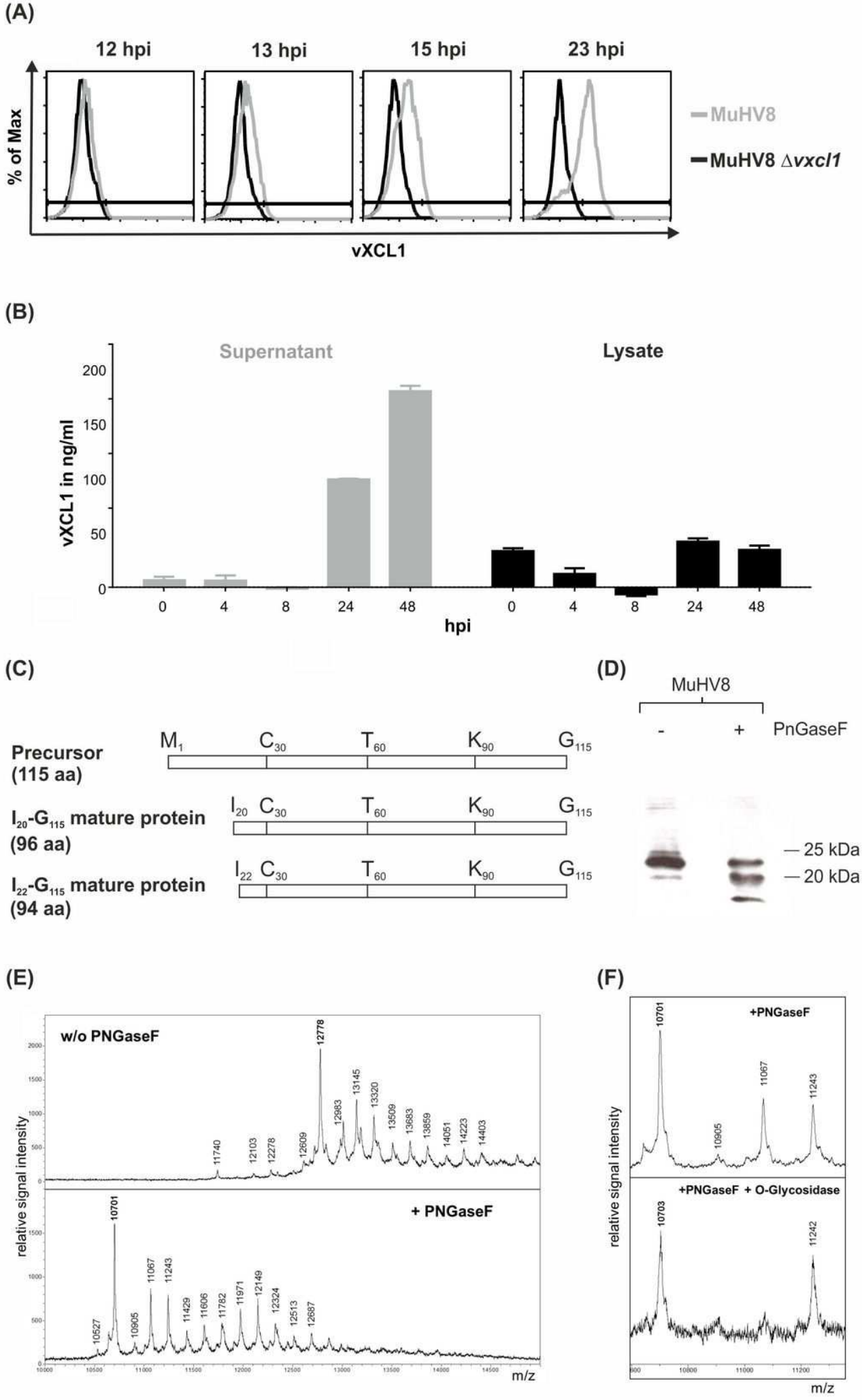
(A)
12 hpi
13 hpi
15 hpi
23 hpi
% of Max
vXCL1
MuHV8
MuHV8 Δvxcl1
(B)
Supernatant
Lysate
vXCL1 in ng/ml
200
150
100
50
0
0
4
8
24
48
hpi
(C)
Precursor (115 aa)
I20-G115 mature protein (96 aa)
I22-G115 mature protein (94 aa)
M1
C30
T60
K90
G115
I20
I22
(D)
MuHV8
-
+
PnGaseF
25 kDa
20 kDa
(E)
w/o PNGaseF
+ PNGaseF
relative signal intensity
m/z
11740
12103
12278
12609
12778
12983
13145
13320
13509
13683
13859
14051
14223
14403
10527
10701
10905
11067
11243
11429
11606
11782
11971
12149
12324
12513
12687
(F)
+PNGaseF
+PNGaseF + O-Glycosidase
relative signal intensity
m/z
10701
10905
11067
11243
10703
11242

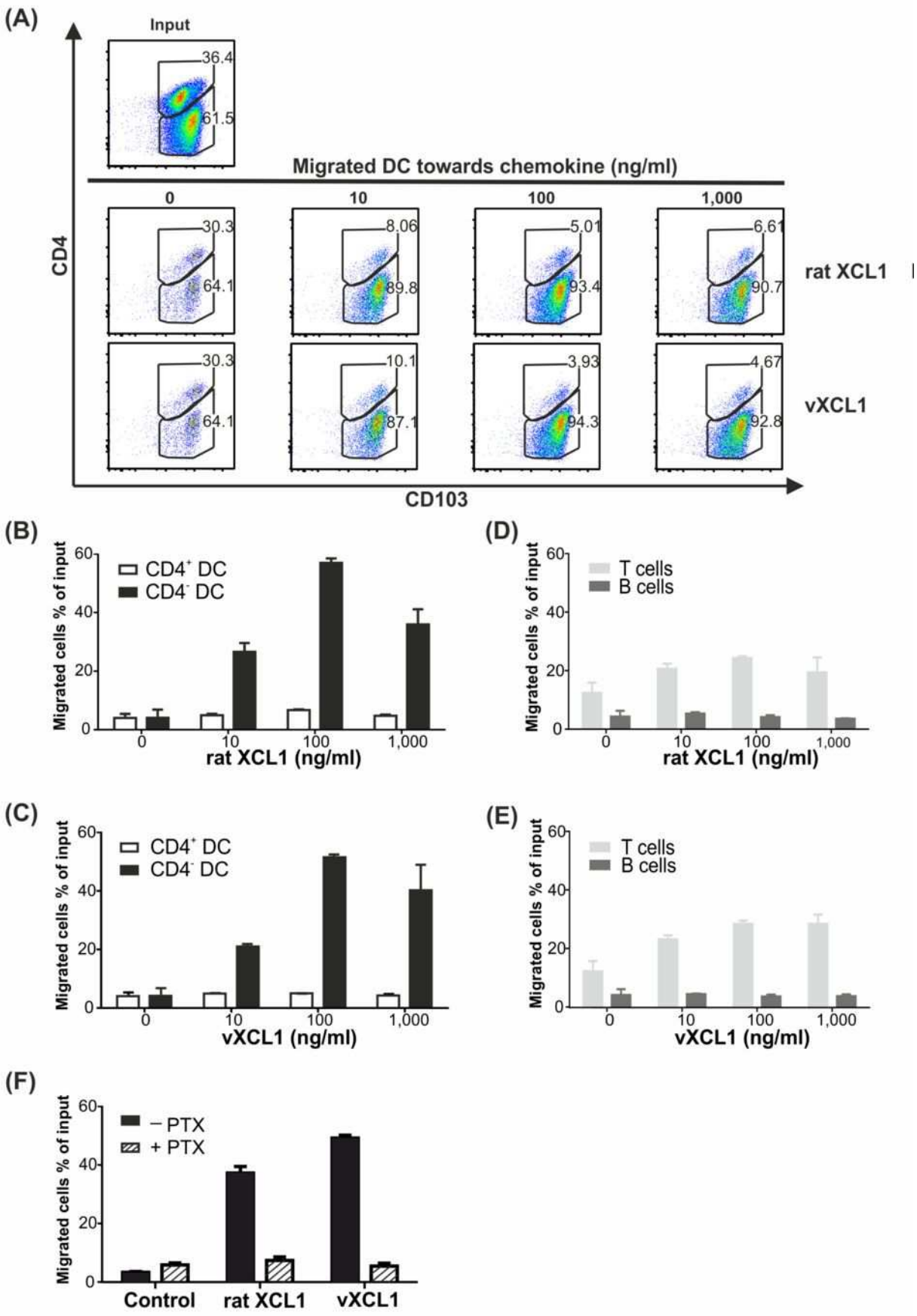
(A)
Input
36.4
61.5
Migrated DC towards chemokine (ng/ml)
0
10
100
1,000
CD4
CD103
30.3
64.1
8.06
89.8
5.01
93.4
6.61
90.7
rat XCL1
30.3
64.1
10.1
87.1
3.93
94.3
4.67
92.8
vXCL1
(B)
Migrated cells % of input
CD4+ DC
CD4- DC
rat XCL1 (ng/ml)
(D)
T cells
B cells
rat XCL1 (ng/ml)
(C)
vXCL1 (ng/ml)
(E)
vXCL1 (ng/ml)
(F)
– PTX
+ PTX
Control
rat XCL1
vXCL1

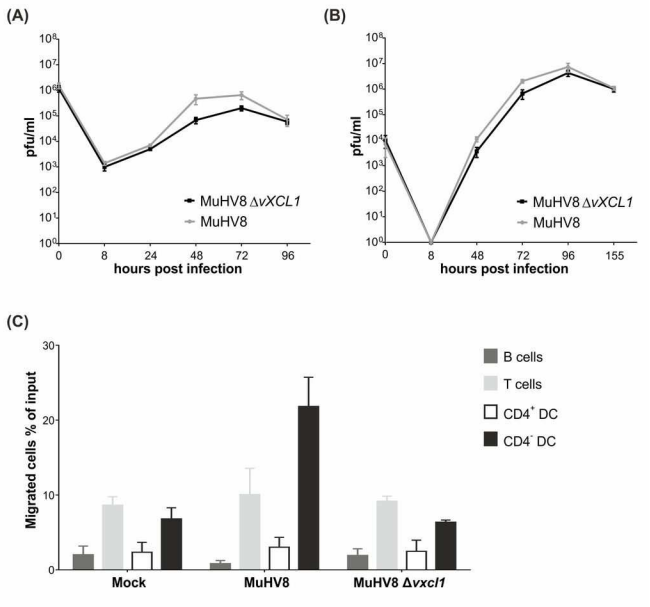
(A)
pfu/ml
hours post infection
MuHV8 ΔvXCL1
MuHV8
(B)
pfu/ml
hours post infection
MuHV8 ΔvXCL1
MuHV8
(C)
Migrated cells % of input
B cells
T cells
CD4+ DC
CD4- DC
Mock
MuHV8
MuHV8 Δvxcl1

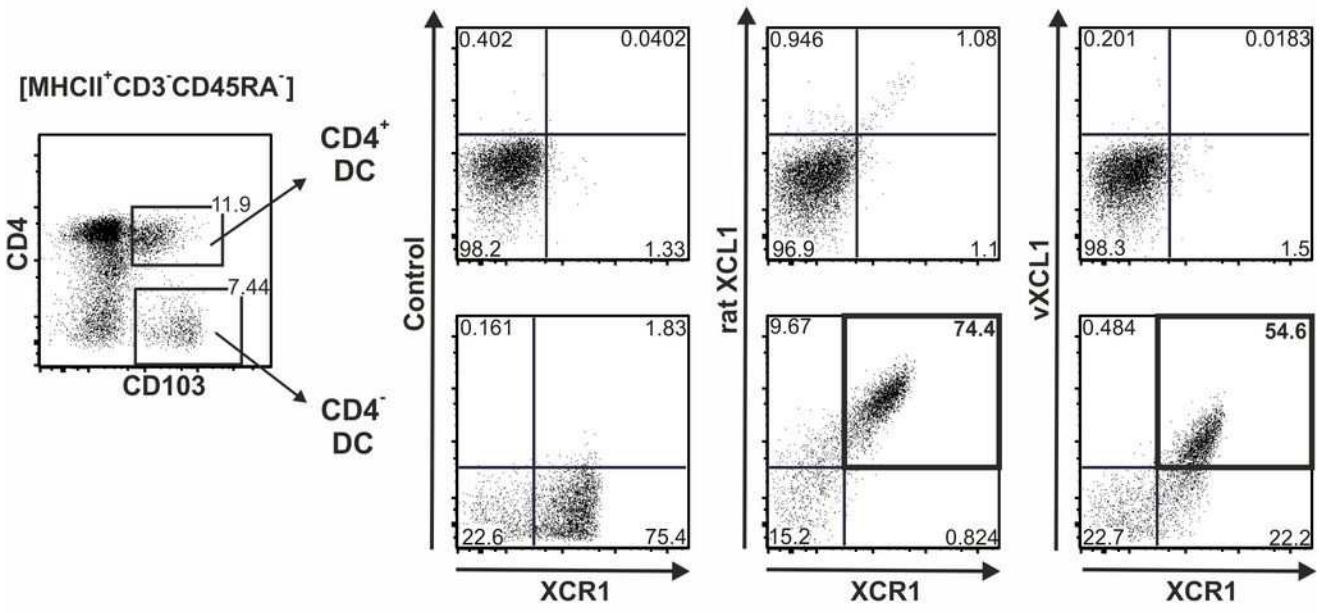
[MHCII+CD3-CD45RA-]
CD4
CD103
11.9
7.44
CD4+ DC
CD4- DC
Control
rat XCL1
vXCL1
0.402
0.0402
98.2
1.33
0.161
1.83
22.6
75.4
0.946
1.08
96.9
1.1
9.67
74.4
15.2
0.824
0.201
0.0183
98.3
1.5
0.484
54.6
22.7
22.2
XCR1
XCR1
XCR1

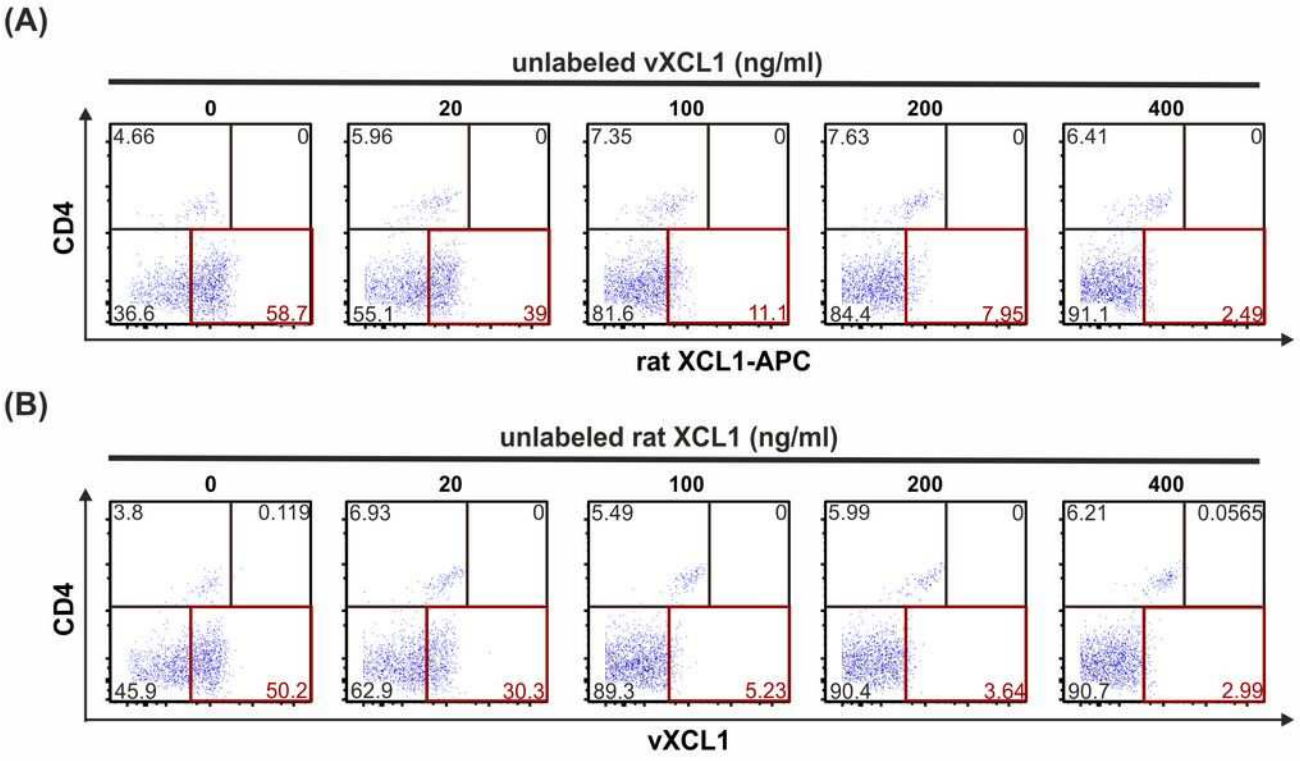
(A)
unlabeled vXCL1 (ng/ml)
0
20
100
200
400
4.66
0
36.6
58.7
5.96
0
55.1
39
7.35
0
81.6
11.1
7.63
0
84.4
7.95
6.41
0
91.1
2.49
CD4
rat XCL1-APC
(B)
unlabeled rat XCL1 (ng/ml)
0
20
100
200
400
3.8
0.119
45.9
50.2
6.93
0
62.9
30.3
5.49
0
89.3
5.23
5.99
0
90.4
3.64
6.21
0.0565
90.7
2.99
CD4
vXCL1